



## Deployment and Exploration of a Gas Storage Well Pattern Based on the Threshold Radius

TANG Ligen<sup>1,2</sup>, ZHU Weiyao<sup>1,\*</sup>, ZHU Huayin<sup>2</sup>, SUN Chunhui<sup>2,3</sup>, YANG Fenglai<sup>4</sup>, WANG Yan<sup>5</sup>, Li Xiaorui<sup>4</sup>, Li Haiming<sup>4</sup>, CHU Guangzhen<sup>2</sup>, WANG Jieming<sup>2</sup>, KONG Debin<sup>1</sup>, YUE Ming<sup>1</sup>, LIU Yuwei<sup>1</sup> and HUANG Kun<sup>1</sup>

<sup>1</sup> University of Science and Technology Beijing, Beijing 100083, China

<sup>2</sup> Research Institute of Petroleum Exploration and Development, CNPC, Beijing 100083, China

<sup>3</sup> Petro China Liaohe Oilfield Company, Panjin, Liaoning 124000, China

<sup>4</sup> Petro China Tarim Oilfield Company, Korla, Xinjiang 841000, China

<sup>5</sup> Petro China Southwest Oil and Gas Field Company, Chongqing 401121, China

**Abstract:** To tackle the problem that wells that are deployed in a specific pattern based on the requirements of gas reservoir development are not suitable for gas storage, we have conducted concentric circular injection and production simulation experiments for gas storage, discovered the existence of a threshold radius, denoted by  $R_t$ , and derived the expression for  $R_t$ . Based on the analysis and discussion results, we propose a strategy for deploying gas storage wells in specific patterns. The expression for  $R_t$  shows that it is affected by factors such as the gas storage gas production/injection time, the upper pressure limit, the lower pressure limit, the bottomhole flow pressure at the ends of injection and production, the and permeability. The analysis and discussion results show that the  $R_t$  of a gas storage facility is much smaller than the  $R_t$  for gas reservoir development. In the gas storage facilities in China, the  $R_t$  for gas production is less than the  $R_t$  for the gas injection, and  $R_t$  increases with the difference in the operating pressure and with permeability  $K$ . Based on the characteristics of  $R_t$ , we propose three suggestions for gas storage well pattern deployment: (1) calculate  $R_t$  according to the designed functions of the gas storage facility and deploy the well pattern according to  $R_t$ ; (2) deploy sparser, large-wellbore patterns in high-permeability areas and denser, small-wellbore patterns in high-permeability areas; and (3) achieve the gas injection well pattern by new drilling, and the gas production well pattern through a combination of the gas injection well pattern and old wells. By assessing a gas storage facility with a perfect well pattern after a number of adjustments, we found that the  $R_t$  of the 12 wells calculated in this paper is basically close to the corresponding actual radius, which validates our method. The results of this study provide a methodological basis for well pattern deployment in new gas storage construction.

**Key words:** gas storage, well deployment strategy, gas injection well pattern, gas production well pattern, threshold radius

Citation: Tang et al., 2021. Deployment and Exploration of a Gas Storage Well Pattern Based on the Threshold Radius. Acta Geologica Sinica (English Edition), 95(2): 630–637. DOI: 10.1111/1755-6724.14655

### 1 Introduction

According to the statistics released by the International Natural Gas Union in 2018 (Kong, 1999; Ladislav, 2018), there are 689 underground gas storage facilities and  $4170 \times 10^8 \text{ m}^3$  of working gas in the world, including 25 storage facilities and  $105 \times 10^8 \text{ m}^3$  of working gas in China. In recent years, with the development of gas storage facilities in China, the current working gas volume has doubled since 2015, and most of the newly added working gas comes from gas reservoir-type gas storage facilities (Tang et al., 2014; Zou et al., 2018). However, although a large volume of working gas is stored underground (Qiao et al., 2017; Li et al., 2018; Chen et al., 2018), it cannot be withdrawn and supplied to the market in a short time period when gas shortages occur, resulting in a situation in

which the stored gas cannot be delivered, and making the role of gas reservoirs not fully effective.

In fact, the situation in which the stored gas cannot be delivered is closely related to the gas storage well patterns, this is because the movement of each party's gas in and out of a gas storage facility is accomplished using wells organized in a specific pattern (Tang et al., 2016a). In the deployment of a gas storage well patterns of gas reservoirs converted into gas storage facilities, because there are few technical reports specifically about gas storage well patterns, gas reservoir development concepts have been primarily used (Yu et al., 2013; Jia et al., 2017; Chen and Wen, 2017; Ma et al., 2018; Liu et al., 2020; Xie et al., 2020). These concepts include an empirical estimation based on 30–50% of the open flow capacity, arranging the wells uniformly in areas with good physical properties without considering heterogeneity, and even the direct use of well spacings in a gas reservoir development. Well

\* Corresponding author. E-mail: weiyao@sina.com

patterns that are arranged in accordance with the gas reservoir development concepts often fail to fully realize the expected working gas volume during the operation of the gas storage facility (Lai et al., 2011; Wu et al., 2012), resulting in the failure of the gas storage facility to perform effectively. The reason why a gas reservoir development well pattern is not suitable for a gas storage facility is that the production conditions of gas storage and gas reservoir development differ in the following aspects. (1) The production time is different. Compared with the 20–30 years for gas reservoir development, gas storage facilities have a strict gas production time limit, i.e., 150 days in the north and 120 days in the south. (2) The average pressures at the end of production are different. The average pressure at the end of production for gas reservoir development is generally close to exhaustion (or a pressure coefficient of 0.1). In contrast, in order for a gas storage facility to maintain continued operation in the later stage, the average pressure at the end of production cannot be lower than a specified value, i.e., the lower pressure limit  $P_{\min}$ .  $P_{\min}$  is generally much higher than the pressure coefficient of 0.1. (3) Their bottomhole flow pressures at the end of production are different. The bottomhole flow pressure in gas reservoir development is generally close to exhaustion. However, due to post-processing and output needs, a gas storage facility generally has strict requirements for the bottomhole flow pressure, which cannot be too low; otherwise, cryogenic treatment and increased output need to be initiated, which increases operating costs. The above three differences, referred to as the constraints of gas production from a gas storage facility, are the main reasons why gas reservoir development well patterns are not suitable for gas storage facilities. The question is what types of well patterns are suitable for gas storage facilities.

In this study, with the goal of solving the gas storage well pattern problem, we designed an experiment, derived expressions for the gas storage well pattern control range, analysed the gas storage well pattern deployment strategies, and developed a technique for future gas storage well pattern deployment.

## 2 Identification of the Radius Threshold

A qualified gas storage well should be able to deliver the expected gas injection and production volumes in accordance with the constraints of the gas storage facility. According with the principle of material balance (Tang et al., 2016b), these expected gas injection and production volumes are governed by the formation supply of this well. Therefore, to qualify a gas storage well, it is necessary to match the appropriate formation supply. In order to explore the formation supply of a gas storage well, we designed an experiment with a concentric circular-core model, simulated a gas storage well, withdrew gas at a set time, and investigated the formation area size that is suitable for the well.

In the experiment, the core model consisted of five steel rings (Fig. 1), equipped with built-in sealed sliding switches and pressure sensors. The core material was homogeneous. The detailed parameters are presented in

Table 1. The constraint of the gas production of the gas storage facility was set as follows. The gas production time was  $t_l = 206$  s, the average pressure in the supply range before gas production (i.e., the upper pressure limit  $P_{\max}$ ) was 3 MPa, and the average pressure in the supply range at the end of gas production (i.e., the lower pressure limit  $P_{\min}$ ) was 2 MPa. The bottomhole flow pressure was  $P_{\text{wff}} \geq 1.1$  MPa at the end of gas production. Five radii were selected. According to the principle of material balance, the gas production rate was calculated based on  $t_l$ . The boundary pressure  $P_e$ , the bottomhole pressure  $P_{\text{wf}}$ , and the balanced average pressure  $P_{\text{av}}$  were recorded at the end of production. The relationships between the model radius and the pressures after gas production are plotted on a semi-logarithmic scale in Figure 2.

The experimental results show that after the gas is produced at a constant rate for 206 s, at all five radii, the results for whether the gas storage constraints are met ( $P_{\text{wff}} \geq 1.1$  MPa and  $P_{\text{av}} = P_{\min}$ ) fall into three cases. The first case is that the models with radii of R1 and R2 satisfy the gas storage constraints, with  $P_{\text{av}}$  after gas production being close to  $P_{\min}$  (2 MPa) and  $P_{\text{wf}}$  being much greater than  $P_{\text{wff}}$  (1.1 MPa). The second case is that the model with a radius of R3 satisfies the gas storage constraints, with  $P_{\text{av}}$  after gas production being similar to  $P_{\min}$  and  $P_{\text{wf}}$  being almost equal to  $P_{\text{wff}}$ . The third case is that the models with radii of R4 and R5 do not meet the gas storage constraints because after gas production,  $P_{\text{av}}$  is greater than  $P_{\min}$  and  $P_{\text{wf}}$  is much smaller than  $P_{\text{wff}}$ .

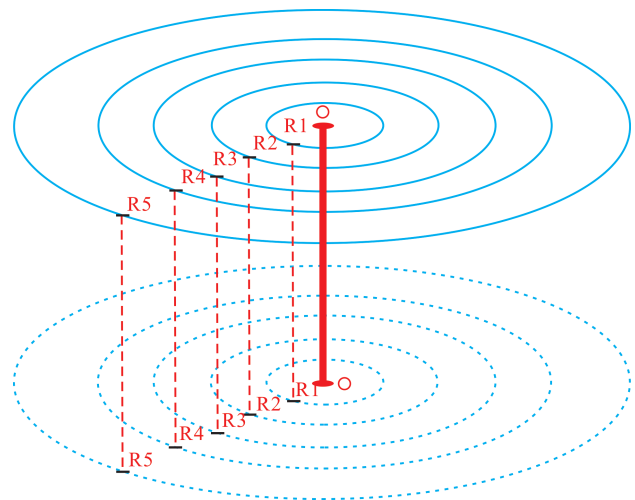


Fig. 1. Schematic diagram of the concentric circular-core model.

Table 1 Basic parameters of the concentric circular-core model

Parameter	Value	Parameter	Value
Model thickness	0.07 m	Radius of the fourth circle R4	0.3 m
Radius of the first circle R1	0.01 m	Radius of the fifth circle R5	0.9 m
Radius of the second circle R2	0.05 m	Porosity	0.06
Radius of the third circle R3	0.1 m	Permeability	0.01 mD

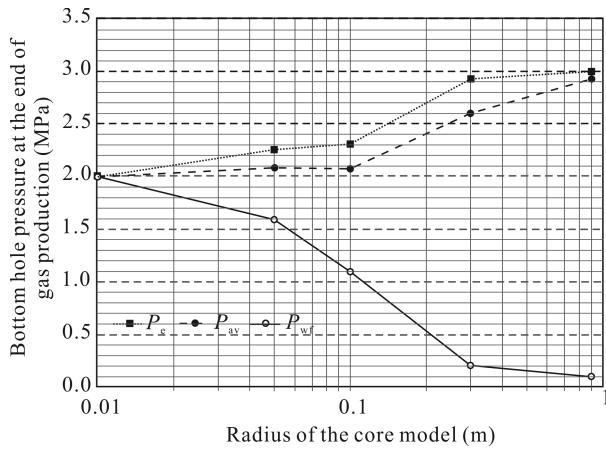


Fig. 2 Semi-logarithmic curves of the relationships between the model radius and the pressures after gas production.

Under the gas storage constraints, there is a limit to the suitable supply radius of a well. The limit seems to be near R3. Because the models with radii of R1, R2, and R3 all meet the gas storage constraints, that is, the formations with radii of R1, R2, and R3 allocated to gas storage wells are all qualified, but R1 and R2 do not perform to the full capacity and would ideally be a bit larger. Once the radius exceeds R3 (i.e., R4 and R5), the gas storage constraints can no longer be met. Therefore, R3 is the limit, which is defined as the threshold radius.

In fact, the existence of a threshold radius is due to the unique gas storage constraints. In the process of estimating the threshold radius, the set values of the equilibrium pressure at the end of gas production and the bottomhole pressure at the end of gas production are also considered. In addition, the basic experimental data used to determine the threshold radius were all obtained through testing under the premise of a gas recovery time limit of 206 s. Thus, parameters such as the gas production time limit and the pressure state after gas production are the main factors affecting the threshold radius. These factors are precisely the differences between gas storage and gas reservoir development. The existence of a threshold radius for a gas storage wells is the result of the unique gas production conditions. The calculation and utilization of the threshold radius were investigated as follows.

### 3 Derivation of the Threshold Radius

To describe the gas storage threshold radius  $R_t$  mathematically, the following assumptions were made. (1) The formation supply range is a closed circular stratum centered on the wellbore. (2) The reservoirs within the supply range are homogeneous and equal in thickness. (3) The reservoirs are connected internally, and there is no impermeable area. (4) Gas production occurs under the bottomhole conditions of a constant flow rate. (5) The gas phase flows in a single phase within the formation supply range, and a small amount of the water or oil components can condense in the gas phase.

According to the definition of and assumptions for  $R_t$ , the permeation process of a gas storage well in its

formation supply range can be simplified as a gas production problem at a constant flow rate in a well at the center of a circular closed boundary. Based on this combined with the inner boundary conditions, the closed outer boundary conditions, and the initial conditions at a constant production rate, comprehensive permeation differential Equation (1) can be obtained (Dake, 1998; Sun, 2015).

$$\begin{cases} \frac{\partial^2 P_p}{\partial r^2} + \frac{1}{r} \frac{\partial P_p}{\partial r} = \frac{\phi \mu c_t}{K} \frac{\partial P_p}{\partial t}, & r_w < r < R_t, t > 0 \\ r \left. \frac{\partial P_p}{\partial r} \right|_{r=r_w} = \frac{Q \mu}{2\pi K h}, & r, t > 0 \\ \left. \frac{\partial P_p}{\partial r} \right|_{r=R_t} = 0, & t > 0 \\ P_p(r, t)_{t=0} = P_{p_{\max}}, & r_w \leq r \leq R_t, t = 0 \end{cases} \quad (1)$$

To solve for the definite solutions, we conducted successive nondimensionalization and a Laplace transform and obtained the analytical solution for the Laplace space:

$$\bar{\varphi}_{Dp}(r_D, t_D) = \frac{[K_1(R_{eD}\sqrt{s})I_0(r_D\sqrt{s}) + I_1(R_{eD}\sqrt{s})K_0(r_D\sqrt{s})]}{s^{3/2}[I_1(R_{eD}\sqrt{s})K_0(\sqrt{s}) - K_1(R_{eD}\sqrt{s})I_1(\sqrt{s})]} \quad (2)$$

The inverse Laplace transform of Equation (2) via the residue method yields the dimensionless pressure at an arbitrary position and time within the supply range:

$$\begin{aligned} \varphi_{Dp}(r_D, t_D) &= \frac{2t_D}{R_{tD}^2 - 1} + \frac{R_{eD}^2}{R_{tD}^2 - 1} \left( \ln \frac{R_{tD}}{r_D} + \frac{r_D^2}{2R_{tD}^2} \right) \\ &\quad - \frac{3R_{tD}^4 - 4R_{tD}^2 \ln R_{tD} - 2R_{tD}^2 - 1}{4(R_{tD}^2 - 1)^2} \\ &\quad - \pi \sum_{n=1}^{\infty} \frac{e^{a_n^2 t_D} J_1^2(R_{eD} a_n) [N_1(a_n) J_0(r_D a_n) - J_1(a_n) N_0(r_D a_n)]}{a_n [J_1^2(R_{eD} a_n) - J_1^2(a_n)]} \end{aligned} \quad (3)$$

It should be noted that in the bottomhole,  $r_D = 1$ . Substituting this into Equation (3) and keeping the first term of the series yields the bottomhole pseudo pressure (Eq. 4) after rearrangement:

$$\begin{aligned} (P_{p_{\max}} - P_{pwf}) \frac{\pi K h T_{sc}}{P_{sc} Q_{sc} T} &= \\ \frac{2t}{R_t^2} \frac{K}{\phi \mu c_t} + \ln \frac{R_t}{r_w} - \frac{3}{4} - 0.84e^{-14.682} \frac{Kt}{\phi \mu c_t h R_t^2} \end{aligned} \quad (4)$$

Further, solving the surface integral of Equation (3) and dividing the result by the supply area yields the average pressure (Eq. 5) within the supply range:

$$P_{\max} - P_{\min} = \frac{Q_{sc} t p B g}{\pi \phi c_t h R_t^2} \quad (5)$$

In this study, we combined Equations (5) and (4) to remove  $Q_{sc}$  and to obtain the threshold radius  $R_t$  of the gas storage facility for gas production:

$$\left[ \frac{(P_{P_{\max}} - P_{P_{wf}})B_g T_{sc}}{P_{sc}(P_{\max} - P_{\min})T} - 2 \right] \frac{K t_p}{\phi \mu c_t R_t^2} = \ln \frac{R_t}{r_w} - \frac{3}{4} - 0.84e^{-14.682 \frac{K t_p}{\phi \mu c_t R_t^2}} \tag{6}$$

Referring to the above process, we also derived the permeation problem during the gas injection process and obtained the threshold radius  $R_t$  for gas injection:

$$\left[ \frac{(P_{P_{wf}} - P_{P_{\max}})B_g T_{sc}}{P_{sc}(P_{\max} - P_{\min})T} - 2 \right] \frac{K t_i}{\phi \mu c_t R_t^2} = \ln \frac{R_t}{r_w} - \frac{3}{4} - 0.84e^{-14.682 \frac{K t_i}{\phi \mu c_t R_t^2}} \tag{7}$$

Though theoretical derivations, we obtained the expressions for the threshold radius  $R_t$ , where Equation (6) expresses the  $R_t$  for gas production and Equation (7) expresses the  $R_t$  for gas injection. However, these expressions are not explicit forms of  $R_t$ , and the input of relevant parameters is required, and as such, the value of  $R_t$  can be solved iteratively or graphically (Lin et al., 2018; Yang et al., 2018; Tang et al., 2020).

As can be seen from the expressions for  $R_t$ , multiple parameters have impacts on the value of  $R_t$ , including the production time  $t$  (gas production time  $t_p$  or gas injection time  $t_i$ ), the upper pressure limit  $P_{\max}$ , the lower pressure limit  $P_{\min}$ , the bottomhole pressure  $P_{wf}$ , the permeability  $K$ , and the other physical parameters for the rock. We analyse and discuss the effects of these parameters on  $R_t$  below.

#### 4 Analysis and Discussion

The above derivation results show that there are many factors affecting  $R_t$ . In order to explore the characteristic of  $R_t$ , two schemes were designed to simulate the requirements of  $R_t$  for different gas injection and production functions of a gas storage facility and the influence of the bottomhole conditions on  $R_t$  at the ends of injection and production. The parameters are described in Table 2.

Scheme 1: Different gas production times were used to simulate the effects of different gas storage functions on

**Table 2** Parameter values used in the threshold radius simulation of  $R_t$

Parameter	Scheme 1	Scheme 2
$P_{\max}$	30 MPa	
$P_{\min}$	13 MPa	
$T$	85°C	
$\phi$	0.2	
$R_g$	0.7	
$R_w$	0.1 m	
$K$	5/15/25/55/105 mD	
$t_p$	90/120/150/365/3650/7300 d	120 d
$t_i$	/	220 d
		Gas production: 12.9/12/11/10/9/8/7/6/5/4/3/2/1/0.1 MPa
$P_{wf}$	13 MPa	Gas injection: 42.9/42/41/40/39/38/37/36/35/34/33/32/31/30.1 MPa

$R_t$ . These gas production times included six gas production conditions: 90 d for emergency peak shaving gas production, 120 d for gas production in the southern regions, 150 d for gas production in the northern regions, 365 d for strategic reserve gas production, 10 years for gas production, and 20 years for gas production. We substituted the parameters for Scheme 1 (Table 2) into Equation (6) to obtain the values of  $R_t$  under different gas production conditions. The relationship curves for  $R_t$  under various gas production conditions are shown in Figure 3.

Scheme 2: Different bottomhole conditions at the ends of injection and production were used to simulate the effects of different injection and production conditions on  $R_t$ . At the end of gas production, based on the different requirements for gas production, processing, and delivery,  $P_{wf}$  values of 13 MPa to 0.1 MPa were used to simulate the operating conditions. At the end of gas injection, based on the conditions of the gas injection compressor,  $P_{wf}$  values of 43 MPa to 30.1 MPa were used to simulate the operating conditions. By substituting the parameters of Scheme 2 (Table 2) into Equations (6) and (7), the  $R_t$  values under the gas injection and gas production conditions were obtained, respectively. The relationships between  $R_t$  and the bottomhole pressure at the ends of gas injection and production are shown in Figure 4.

By analyzing the simulation results for Scheme 1 and Scheme 2, it was found that because it is affected by the

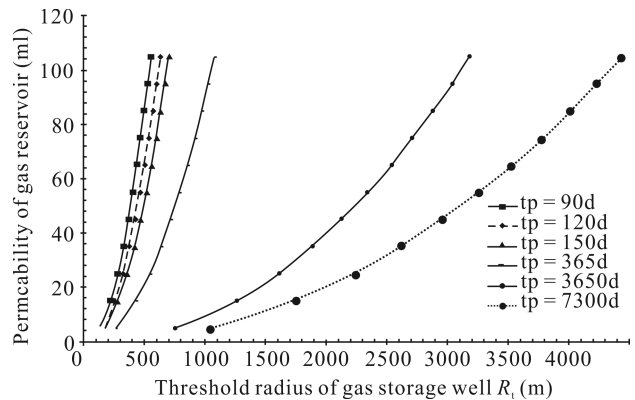


Fig. 3. Relationships between the threshold radius  $R_t$  and the operating conditions for different gas storage functions.

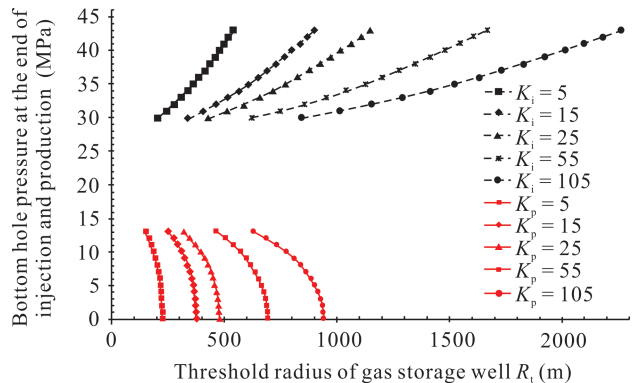


Fig. 4. Relationships between the threshold radius  $R_t$  and the bottomhole pressures at the ends of injection and production ( $K_i$  for gas injection,  $K_p$  for gas production).

gas storage constraints,  $R_t$  exhibits different trends, which are mainly represented by the following five aspects.

(1) The  $R_t$  values for gas storage are much smaller than the  $R_t$  values for gas reservoir development. Among the six simulated gas storage functions, the  $R_t$  of the 90 d emergency peak shaving gas production is the smallest and is located at the far left in Figure 3. As the gas production time increases, the  $R_t$  curves for the 120 d and 150 d production times shift to the right in turn, and the  $R_t$  curve for the 365 d production time shifts to the right by a larger margin. However, the value of  $R_t$  does not exceed 1200 m under these gas production operating conditions. As the gas production time increases to 10 and 20 years, these time scales exceed the range of normal gas storage facilities and are almost close to the gas production time of gas reservoir development. In these cases, the  $R_t$  curves continue to shift to the right by a large margin and can reach as far as 4500 m at high permeabilities. For example, if a gas storage well pattern is deployed based on the idea of gas reservoir development, that is, the well pattern of a gas storage facility intended to accommodate 90 d emergency peak shaving is deployed based on the 4500 m radius intended for a 20 year gas reservoir development production time, the deployed wells will be unqualified and cannot accomplish the 90 d gas production required for emergency peak shaving.

(2)  $R_t$  has a maximum value and a minimum value. Figure 4 shows the upper and lower  $R_t$  curves, where the upper black  $K_i$  represents the  $R_t$  for gas injection, and the lower red  $K_p$  represents the  $R_t$  for gas production. The gas injection  $R_t$  curve has a minimum value at the lower end. Because it is close to the upper pressure limit of 30 MPa for gas storage, there is almost no room for manual control and adjustment. The gas injection  $R_t$  curve has a maximum value at the upper end. If the pressure of the surface compressor and the pressure bearing capacity of the formation are high enough, this value may increase further, which allows room for manual manipulation. Contrary to the  $R_t$  for gas injection, the gas production  $R_t$  curve has a minimum value at the top of the curve and a maximum value at the bottom of the curve. Because the minimum value is close to the lower pressure limit of 13 MPa for gas storage, and the maximum value is close to atmospheric pressure (0.1 MPa), there is almost no room for manual adjustment and control.

(3)  $R_t$  increases as the operating pressure difference increases. In Scheme 2, by setting the bottomhole pressures at the ends of gas injection and production, the injection pressure difference ( $P_{wf} - P_{max}$  for gas injection) is equal to the production pressure difference ( $P_{min} - P_{wf}$  for gas production), so the simulated  $R_t$  for gas injection and the  $R_t$  for gas production are more comparable. Taking a permeability of 5 mD as an example, as the gas injection pressure difference increases from bottom to top, the  $R_t$  curve for the gas injection extends toward the upper right. Similar behaviours occur for other permeabilities. As the gas production pressure difference increases from top to bottom, the  $R_t$  curves for gas production increase toward the lower right. The operating pressure difference affects the value of  $R_t$  to a certain extent, but it has a limited effect on low-permeability reservoirs. Therefore, it is not

recommended that low-permeability gas storage facilities be equipped with high-grade compressors or use an increased pressure differential for gas production.

(4) The  $R_t$  for gas production is smaller than the  $R_t$  for gas injection. When the gas production pressure difference is equal to the injection gas pressure difference, the simulated  $R_t$  for gas production is less than that for gas injection. Moreover, as the production pressure difference increases, the difference between the  $R_t$  for gas production and the  $R_t$  for gas injection is more noticeable in high-permeability gas storage facilities than in low-permeability gas storage facilities, as is shown in Figure 4 for a permeability of 105 mD.

(5)  $R_t$  increases with increasing formation permeability. As is shown in Figure 3, as the permeability increases, the  $R_t$  for gas production increases continuously. This behaviour occurs for all of the storage functions. In Figure 4, as the permeability increases, the  $R_t$  curves shift from left to right with continuously increasing values. Both the  $R_t$  curves for gas production and the  $R_t$  curves for gas injection exhibit this behaviour.

## 5 Idea of Gas Storage Well Pattern Arrangement

$R_t$  is calculated according to the designed gas storage function, and a well pattern that matches its function is deployed according to the calculated  $R_t$ . Because the gas storage  $R_t$  is much smaller than the gas reservoir  $R_t$ , if a gas reservoir development well pattern is deployed for a gas storage facility, the well pattern cannot completely control the gas storage layers, resulting in insufficient utilization of some of the reservoirs and difficulty in meeting the expected injection and production demands, or in unqualified gas storage wells. Similarly, if a well pattern designed for a 150 d gas production period is deployed for a gas storage facility built to accommodate 90 d emergency peak shaving, because the  $R_t$  values of the two production periods are different, it is impossible to achieve the expected emergency peak shaving goal. Therefore, to achieve the expected functions of a gas storage facility, it is recommended to convert the gas storage functions into the gas storage constraints, substitute them into the  $R_t$  expressions derived in this paper to calculate the matching  $R_t$  values, control the formation range according to the calculated  $R_t$ , and deploy the well pattern matching the anticipated functions of the gas storage facility.

To achieve efficient production from the entire gas storing formation, it is recommended to deploy sparser, large-wellbore patterns in high-permeability areas and denser, small-wellbore patterns in low-permeability areas. The analysis results show that the  $R_t$  for a high-permeability area is greater than the  $R_t$  for a low-permeability area. In other words, the control range of a high-permeability well is larger than that of a low-permeability well. If the formation in the same area is to be controlled, the number of wells required for the high-permeability-area is smaller and the number of wells required for the low-permeability area is larger. Furthermore, based on the principle of material balance, the productivity of wells in high-permeability areas are

higher than those of wells in low-permeability areas. Thus, to deliver gas to the wellhead, the wellbore size needs to be larger. The wellbore size required in the low permeability area is smaller. Therefore, it is recommended that sparser, large-wellbore patterns be deployed in high-permeability areas and denser, small-wellbore patterns be deployed in low-permeability areas.

To reduce the investment, gas injection well patterns are realized through new drilling, and gas production well patterns are realized through a combination of gas injection well patterns and old wells. Currently, gas storage facilities in China are designed according to 120 d and 150 d gas production periods. Based on the simulation results of Scheme 2, the  $R_t$  for gas injection in these two types of gas storage facilities is greater than the  $R_t$  for gas production. This means that for the same well, the range of the formation control is greater for gas injection than for gas production. To achieve the expected gas production function of a gas storage facility, the number of gas injection wells required is less than the number of gas production wells required. Because they need to sustain the special operating conditions of high temperature, high pressure, and alternating loads, gas injection wells are required be of a higher quality and they are generally newly drilled wells. The finished wells are able to perform the functions of gas injection and production wells and to complete all of the gas injection tasks and some of the gas production tasks. The question remains of whether or not the remaining wells needed for performing gas production need to be newly drilled. For new drilling, a large investment is required, and an additional investment is required to plug the old wells. However, there is an alternative that does not require new drilling and that uses the old wells to assist in the gas production. There are many old wells drilled prior to the construction of a gas storage facility. These wells do not meet the requirements of gas injection wells; however, because gas the production operation has lower operating requirements than the gas injection operation, some of the older wells that are of a better quality or can be treated can be converted into auxiliary gas production wells. The advantage of using the old wells to complete the remaining gas production functions is that as long as the new drilling meets the gas injection demand, the remaining gas production functions no longer require new drilling, leading to a decreased investment. An additional decrease in investment results from not needing to plug the repurposed old wells. This specific situation depends on whether or not the quality of the old wells meets the gas production requirements. To reduce the investment, it is recommended that new wells be drilled only for the purpose of gas injection. The new wells partially contribute to the gas production functions. The remainder of the gas production functions are supplemented by the old wells left over from the gas reservoir development.

## 6 Filed Verification

The DZ gas storage is one of the oldest commercial gas storage facilities operating in China. In the early construction stage of the DZ gas storage facility, the well

pattern was deployed based on the gas field development concept. After it went into production, it was found that the storage facility had difficulty achieving the expected gas production function. As such, to expand the capacity and increase production, several well pattern densifications were attempted, which have enabled the peak shaving capacity of the gas storage facility to basically meet expectations in recent years. The results of this gas production experience show that the well pattern currently meets the expected function of the gas storage facility. We substituted the present operating conditions of the DZ gas storage facility into Equation (6) to calculate the  $R_t$  of 12 wells (Table 3).

**Table 3 Comparison of  $R_t$  and the corresponding actual radius of the DZ gas storage wells**

Well number	Permeability (mD)	$R_t$ (m)	Measured actual radius (m)	Difference (%)
1	16	312	289	-8
2	25	328	356	7.9
3	36	437	422	-3.6
4	42	447	427	-4.7
5	49	463	488	5.1
6	55	513	484	-6
7	64	583	553	-5.4
8	70	577	542	-6.5
9	81	634	618	-2.6
10	86	626	598	-4.7
11	96	674	629	-7.2
12	100	672	683	2.6

The calculated  $R_t$  and the corresponding actual measured radii are quite similar, with a maximum difference of 8%, which falls within the acceptable range of precision for oil field operations. Such prediction results can be used to design gas storage facilities converted from gas fields. In addition, the difference in the results for nine of the wells was negative, indicating that the actual radii are slightly smaller than the  $R_t$ , and that such a well pattern can cover the gas storage formation completely with some leeway, thereby ensuring that the actual peak shaving capacity meets the expectations.

## 7 Conclusions

Based on the characteristics of gas storage operations, we designed physical simulation experiments, and determined that a gas storage well has a threshold formation control range, which is defined as the threshold radius  $R_t$ . By combining the theory of unstable permeation and the principle of material balance, we derived the expressions for the  $R_t$  of gas storage injection and production wells and determined the influencing factors, such as the gas injection and production time, the upper and lower pressure limits, the bottomhole flow pressures at the ends of injection and production, and the permeability.

We investigated the characteristics of  $R_t$  and concluded that the  $R_t$  for gas storage is much smaller than the  $R_t$  for gas reservoir development, the  $R_t$  for gas injection is greater than the  $R_t$  for gas production, and  $R_t$  increases as the operating pressure difference and permeability increase. Based on this, we provide three

recommendations for developing a gas storage well pattern deployment strategy. (1) Based on the designed function of the gas storage facility, the  $R_t$  should be calculated and the well pattern should be deployed based on the value of  $R_t$ . (2) Sparser, large-wellbore patterns should be deployed in high-permeability areas, and denser, small-wellbore well patterns should be deployed in low-permeability areas. (3) The gas injection well pattern should be implemented by drilling new wells, and the gas production well pattern should be implemented through combination of the gas injection well pattern and old wells.

A case study of the DZ gas storage facility demonstrates that the  $R_t$  derived in this study is consistent with the actual radius, thereby validating the use of  $R_t$  in designing well patterns for gas storage facilities.

### Acknowledgements

We thank relevant managers and experts from the PetroChina Exploration and Development Research Institute for their unreserved guidance. This work is granted by the National Key Research and Development Project grant number 2017YFC0805801 and the Chinese Academy of Engineering Major Consulting Project grant number 2017-ZD-03.

Manuscript received May 20, 2019  
accepted Sep. 29, 2020  
associate EIC: ZHANG Shuichang  
edited by FANG Xiang

### Symbols

$P_{\min}$ —lower pressure limit of the gas storage operation (MPa);  
 $P_{\max}$ —upper pressure limit of the gas storage operation (MPa);  
 $t$ —gas production time in the experiment (206 s);  
 $P_{wif}$ —set bottomhole flow pressure at the end of gas production in the experiment (MPa);  
 $P_{wf}$ —actual bottomhole flow pressure at the end of gas production in the experiment (MPa);  
 $P_{av}$ —average product pressure after equilibrium is reached in the experiment (MPa);  
 $R_t$ —threshold radius of the gas storage well as defined in this study (m);  
 $P_p$ —pseudo-pressure ( $\text{MPa}^2/(\text{mPa}\cdot\text{s})$ );  
 $r$ —radius from the center of the borehole (m);  
 $h$ —thickness of the gas storage formation (m);  
 $\varphi$ —porosity of the gas storage formation;  
 $\mu$ —gas viscosity ( $\text{mPa}\cdot\text{s}$ );  
 $c_t$ —comprehensive compressibility ( $\text{MPa}^{-1}$ );  
 $K$ —gas storage formation permeability ( $10^{-3} \mu\text{m}^2$ );  
 $t$ —production time (d);  
 $r_w$ —wellbore radius (m);  
 $R_e$ —formation supply radius of the gas storage well,  $R_e = R_t$  in this study (m);  
 $Q$ —amount of production under the formation conditions ( $\text{m}^3/\text{d}$ );  
 $P_{p\max}$ —the upper pressure limit of the gas storage facility in pseudo-pressure form ( $\text{MPa}^2/(\text{mPa}\cdot\text{s})$ );  
 $\psi_{DP}$ —dimensionless pressure;  
 $t_D$ —dimensionless time;  
 $r_D$ —dimensionless radius from the center of the borehole;  
 $R_{eD}$ —dimensionless radius of formation supply of the gas storage well;  
 $I_0$ —modified Bessel function of the first kind of order 0;  
 $I_1$ —modified Bessel function of the first kind of order 1;  
 $K_0$ —modified Bessel function of the second kind of order 0;  
 $K_1$ —modified Bessel function of the second kind of order 1;  
 $J_0$ —Bessel function of the first kind of order 0;  
 $J_1$ —Bessel function of the first kind of order 1;  
 $N_0$ —Bessel function of the second kind of order 0;  
 $N_1$ —Bessel function of the second kind of order 1;

$P_{p\max}$ —upper pressure limit in pseudo-pressure form ( $\text{MPa}^2/(\text{mPa}\cdot\text{s})$ );  
 $P_{pwr}$ —bottomhole flow pressure in pseudo-pressure form ( $\text{MPa}^2/(\text{mPa}\cdot\text{s})$ );  
 $P_{sc}$ —pressure under standard conditions ( $P_{sc} = 0.101325 \text{ MPa}$ );  
 $Q_{sc}$ —amount of gas production under standard conditions ( $\text{m}^3/\text{d}$ );  
 $T$ —temperature of the gas storage formation (K);  
 $T_{sc}$ —temperature under standard conditions ( $T_{sc} = 293 \text{ K}$ );  
 $B_g$ —gas volume factor of the gas storage facility;  
 $t_p$ —gas production time determined from the gas storage function (d);  
 $P_{pwrif}$ —bottom flow pressure of a gas production well in pseudo-pressure form ( $\text{MPa}^2/(\text{mPa}\cdot\text{s})$ );  
 $P_{pwrif}$ —bottom flow pressure of a gas injection well in pseudo-pressure form ( $\text{MPa}^2/(\text{mPa}\cdot\text{s})$ );  
 $t_{in}$ —gas injection time determined from the gas storage function (d).

### References

- Chen, S.Y., Zhang, Q., Wang, G., Zhu, L.J., and Li, Y., 2018. Investment strategy for underground gas storage facilities based on real option model considering gas market reform in China. *Energy Economics*, 70: 132–142.
- Chen, X.X., and Wen, H., 2017. Evaluation of single gas well production capacity of Shuang-6 gas storage in Liaohe oilfield. *Xinjiang Petroleum Geology*, 38(06): 715–718 (in Chinese with English abstract).
- Dake, L.P., 1998. *Fundamentals of reservoir engineering*. Elsevier: 127–148.
- Jia, A.L., Meng, D.W., He, D.B., Wang, G.T., Guo, J.L., Yan, H.J., and Guo, Z., 2017. Technical measures of deliverability enhancement for mature gas fields: A case study of Carboniferous reservoirs in Wubaiti gas field, eastern Sichuan Basin, SW China. *Petroleum Exploration and Development*, 44(4): 580–589 (in Chinese with English abstract).
- Kong, X., 1999. *Advanced mechanics of fluids in porous media*. Hebei: Press of University of Science and Technology of China, 248–292 (in Chinese).
- Lai, G., Wang, M.X., Kerkre, S., Scheller-Wolf, A., and Secomandi, N., 2011. Valuation of storage at a liquefied natural gas terminal. *Operations Research*, 59(3): 602–616.
- Ladislav, G., 2018. *Underground gas storage 2015–2018 triennium work report*. International Gas Union.
- Li, B.Y., Yin, H.T., and Wang, F., 2018. Will China's "dash for gas" halt in the future? *Resources, Conservation and Recycling*, 134: 303–312.
- Liu, P.C., Yu, H.J., An, H.Y., Xu, W., and Zhu, Y.J., 2020. Optimization design of well pattern in heterogeneous gas storage. *Journal of Southwest Petroleum University (Science and Technology Edition)*, 42(2): 141–148 (in Chinese with English abstract).
- Lin, H.W., Takashi, M., and Deng, C.Y., 2018. Survey on geometric iterative methods and their applications. *Computer-Aided Design*, 95: 40–51.
- Ma, X.H., Zheng, D.W., Shen, R.C., Wang C.Y., Luo, J.H., and Sun, J.C., 2018. Key technologies and practice for gas field storage facility construction of complex geological conditions in China. *Petroleum Exploration and Development*, 45(3): 489–499 (in Chinese with English abstract).
- Qiao, Z., Guo, Q.L., and Sun, H.B., 2017. Optimal gas storage capacity in gas power plants considering electricity and natural gas systems constraints. *Energy Procedia*, 142: 2983–2989.
- Sun, H.D., 2015. *Advanced production decline analysis and application*. Elsevier: 221–262.
- Tang, L.G., Wang, J.M., Bai, F.J., and Shi, L., 2014. Inventory forecast in underground gas storage based on modified material balance equation. *Petroleum Exploration and Development*, 41(4): 480–484 (in Chinese with English abstract).
- Tang, L.G., Wang, J.M., Ding, G.S., Sun, S.S., Zhao, K., and Sun, J.C., 2016a. Downhole inflow-performance forecast for underground gas storage based on gas reservoir development data. *Petroleum Exploration and Development*, 43(1): 127–130 (in Chinese with English abstract).
- Tang, L.G., Sun, S.S., Mi, L.D., Li, H.L., Guo, K., Wang, J.M., and Bai, F.J., 2016b. Method for deliverability prediction of well in gas storage converted from gas reservoir in China. *SPE Asia Pacific Oil and Gas Conference and Exhibition*,

- Perth, Australia.
- Tang, L.G., Zhu, W.Y., Zhu, H.Y., Wang, Y., Jiang, H.Q., Peng, P., Li, D.S., Wang, J.M., Li, C., Yang, Y., Ren, K., Wu, Z.D., and Li, L.M., 2020. Monitoring well pattern deployment in China gas storage and its initial success rate. *Journal of Energy Storage*, online. <https://doi.org/10.1016/j.est.2020.101950>.
- Wu, O.W., Wang, D., and Qin, Z.W., 2012. Seasonal energy storage operations with limited flexibility. *Manufacturing and Service Operations Management*, 13(3): 455–471.
- Xie, J., Pan, Z.P., Wang, Y.Z., Wang, J.M., and Wang, J.K., 2020. The water sand evaluation and capacity expansion for the Ban 876 Underground Gas Reservoir. *Periodical of Ocean University of China*, 50(2): 100–106 (in Chinese with English abstract).
- Yang, L., Sun, Y.Q., and Gong, F.H., 2018. The inexact residual iteration method for quadratic eigenvalue problem and the analysis of convergence. *Journal of Computational and Applied Mathematics*, 332: 45–55.
- Yu, B.F., Yan, X.Z., Yang, X.J., and Wang, T.T., 2013. Dynamic reservoir pressure prediction of depleted reservoir gas storage considering the fractal feature of porous medium. *Acta Petrolei Sinica*, 34(5): 1017–1022 (in Chinese with English abstract).
- Zou, C.N., Yang, Z., He, D.B., Wei, Y.S., Li, J., Jia, A.L., Chen, J.J., Zhao, Q., Li, Y.L., Li, J., and Yang, S., 2018. Theory, technology and prospects of conventional and unconventional

natural gas. *Petroleum Exploration and Development*, 45(4): 1–13 (in Chinese with English abstract).

#### About the first author



TANG Ligen, male, born in 1982 in Heze City, Shandong Province; a doctoral candidate from University of Science and Technology Beijing; Senior Engineer of CNPC. He is now interested in the study on gas storage and its monitoring. Email: [jiazinia4120@126.com](mailto:jiazinia4120@126.com); phone: 010-83599517.

#### About the corresponding author



ZHU Weiyao, male, born in 1960 in Daqing City, Liaoning Province; doctor; graduated from University of Chinese Academy of Sciences; professor of University of Science and Technology Beijing. He is now interested in the study on theoretical research and engineering practice of seepage mechanics and oil and gas field development engineering. Email: [weiyao@sina.com](mailto:weiyao@sina.com); phone: 010-62332778.